Forebrain-selective AMPA-receptor antagonism guided by TARP γ-8 as an antiepileptic mechanism

Akihiko S Kato[1], Kevin D Burris[1], Kevin M Gardinier[1], Douglas L Gernert[1], Warren J Porter[1], Jon Reel[1], Chunjin Ding[1], Yuan Tu[1], Douglas A Schober[1], Matthew R Lee[2], Beverly A Heinz[1], Thomas E Fitch[1], Scott D Gleason[1], John T Catlow[1], Hong Yu[1,4], Stephen M Fitzjohn[3,4], Francesca Pasqui[3], He Wang[1], Yuewei Qian[1], Emanuele Sher[3], Ruud Zwart[3], Keith A Wafford[3], Kurt Rasmussen[1], Paul L Ornstein[1,4], John T R Isaac[3,4], Eric S Nisenbaum[1], David S Bredt[1,4] & Jeffrey M Witkin[1]

Pharmacological manipulation of specific neural circuits to optimize therapeutic index is an unrealized goal in neurology and psychiatry. AMPA receptors are important for excitatory synaptic transmission[1], and their antagonists are antiepileptic[2]. Although efficacious, AMPA-receptor antagonists, including perampanel (Fycompa), the only approved antagonist for epilepsy, induce dizziness and motor impairment[3,4]. We hypothesized that blockade of forebrain AMPA receptors without blocking cerebellar AMPA receptors would be antiepileptic and devoid of motor impairment. Taking advantage of an AMPA receptor auxiliary protein, TARP γ-8, which is selectively expressed in the forebrain and modulates the pharmacological properties of AMPA receptors[5], we discovered that LY3130481 selectively antagonized recombinant and native AMPA receptors containing γ-8, but not γ-2 (cerebellum) or other TARP members. Two amino acid residues unique to γ-8 determined this selectivity. We also observed antagonism of AMPA receptors expressed in hippocampal, but not cerebellar, tissue from an patient with epilepsy. Corresponding to this selective activity, LY3130481 prevented multiple seizure types in rats and mice and without motor side effects. These findings demonstrate the first rationally discovered molecule targeting specific neural circuitries for therapeutic advantage.

Perampanel (Fycompa)[2], which is used to control refractory partial seizures, blocks cerebellar AMPA receptors with similar potency and efficacy as hippocampal receptors, and induces sedation and ataxia in rats and mice and dizziness and falling in patients[3,4]. We developed a high-throughput intracellular-calcium-dye-based assay, FLIPR, to identify compounds that specifically block AMPA receptors associated with TARP γ-8. Glutamate stimulated an increase in calcium flux in CHO-S cells transfected with GluA1-flip (GluA1i) alone or co-transfected with GluA1-flop (GluA1o) and either γ-2 or γ-8. Flip and flop variants are generated by alternative splicing and the gating properties of the variants are different. To normalize the amplitude of calcium influx, we used flip and flop isoforms differentially (Online Methods). Co-application of glutamate with cyclothiazide (CTZ), an AMPA-receptor potentiator, enhanced the response (**Fig. 1a**), consistent with previous electrophysiological findings[5,6]. We detected large kainate-evoked responses in cells expressing GluA1o + γ-2 or GluA1o + γ-8, but not in cells expressing GluA1i alone (**Fig. 1b**), consistent with increased kainate efficacy in the presence of TARPs[7,8]. GYKI53784, which blocks all AMPA-receptor-mediated currents, completely blocked calcium influx in all transfections (**Fig. 1c**).

We then screened several thousand compounds from the Lilly collection for their ability to block glutamate/CTZ-stimulated calcium responses in cells expressing GluA1o + γ-8. Active compounds were examined in cells expressing GluA1i alone and in cells expressing GluA1o + γ-2 to identify TARP-dependent and TARP-subtype-selective activity, respectively. Subsequent chemical structure–activity relationship (SAR) studies led to the discovery of LY3130481 (6-((*S*)-1-{1-[5-(2-hydroxy-ethoxy)-pyridin-2-yl]-1H-pyrazol-3-yl}-ethyl)-3-H-1,3-benzothiazol-2-one), which potently blocked GluA1o + γ-8, but not GluA1i alone or GluA1o + γ-2 (**Fig. 1d**,**e**,**g**). Detailed chemical synthesis and the SAR of LY3130481 have been published previously[9]. LY3130481 is not related to any known category or class of compounds in clinical use. As previously published[10], GYKI53784 inhibited GluA1 receptors without preference for γ-2 versus γ-8 (**Fig. 1f**).

We further explored the pharmacology of LY3130481 using voltage-clamp recordings. Glutamate application on GluA1i-transfected cells evoked inward currents, which rapidly desensitized to a small steady-state current, and TARP co-transfection markedly modified these characteristics (**Supplementary Fig. 1**)[5,11]. LY3130481 potently and efficaciously blocked glutamate-evoked currents in cells transfected with GluA1i + γ-8 (**Fig. 2a**). LY3130481 had minimal effect on the other recombinant channels, with the exception of GluA1i +

[1]Lilly Research Laboratory, Eli Lilly and Company, Indianapolis, Indiana, USA. [2]Applied Molecular Evolution, Eli Lilly and Company, San Diego, California, USA. [3]Lilly UK, Eli Lilly and Company, Windlesham, UK. [4]Present addresses: Janssen PRD, San Diego, California, USA (H.Y. and D.S.B.); School of Physiology, Pharmacology and Neuroscience, University of Bristol, Bristol, UK (S.M.F.); College of Pharmacy, Roosevelt University, Schaumburg, Illinois, USA (P.L.O.); Wellcome Trust, London, UK (J.T.R.I.). Correspondence should be addressed to A.S.K. (katoak@lilly.com) or J.M.W. (jwitkin@lilly.com).

Received 5 February; accepted 30 September; published online 7 November 2016; doi:10.1038/nm.4221

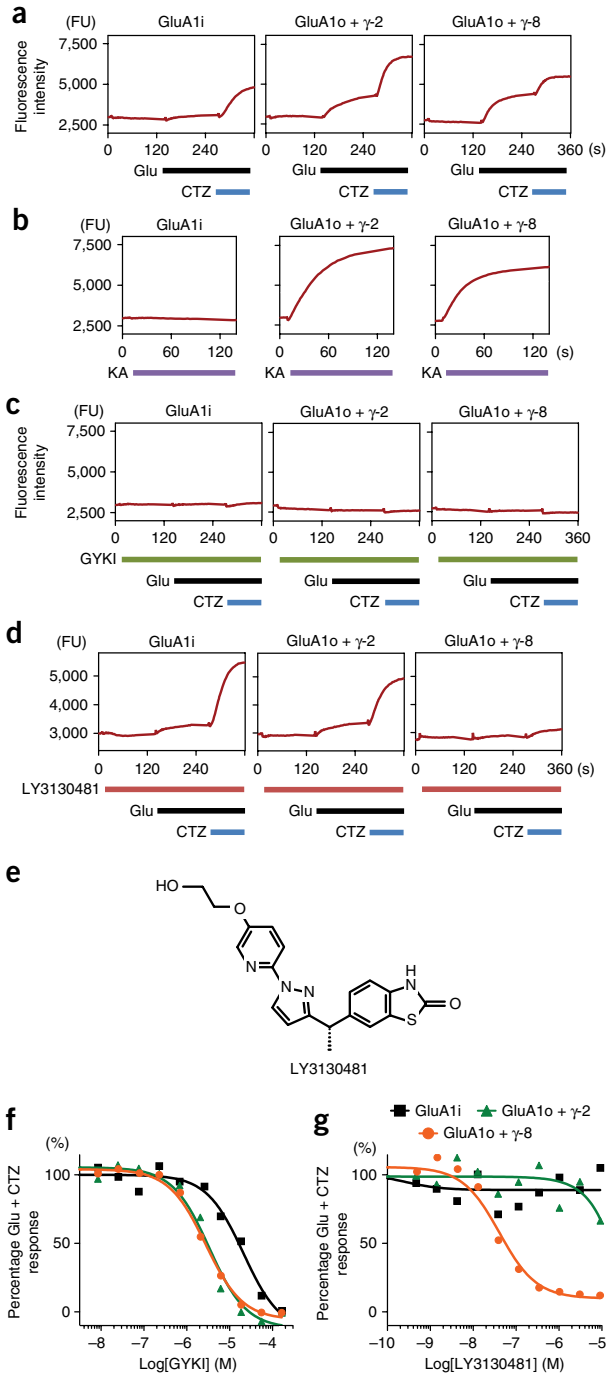

Figure 1 Identification of γ-8-selective AMPA-receptor antagonists. (**a**–**d**) Representative time courses in which $[Ca^{2+}]_i$ was measured in Fluo-4-a.m.-loaded CHO-S cells transfected with GluA1i alone, GluA1o + γ-2 or GluA1o + γ-8 using the FLIPR multi-well calcium system (Online Methods). Bars below the graphs indicate the timing of compound application. Final compound concentrations: glutamate (5 μM) and then glutamate (45 μM) + CTZ (20 μM); kainate (15 μM); GYKI (167 μM); LY3130481 (9.3 μM). FU, fluorescence unit. (**e**) The chemical structure of LY3130481, 6-((*S*)-1-{1-[5-(2-hydroxy-ethoxy)-pyridin-2-yl]-1H-pyrazol-3-yl}-ethyl)-3- H-1,3-benzothiazol-2-one. [US patent 8,765,960]. (**f**,**g**) Concentration-response curves for GYKI53784 (**f**) and LY3130481 (**g**) against the glutamate + CTZ responses. Data in **f** and **g** are shown as representative experiments (GYKI: GluA1i, $n = 275$ assays; GluA1o + γ-8, $n = 157$; GluA1o + γ-2 = 274; LY3130481: GluA1i, $n = 26$; GluA1o + γ-8, $n = 30$; GluA1o + γ-2 = 28).

γ-4 (the closest γ-8 homolog)[5], for which it displayed ~100-fold lower potency. LY3130481 also had no effect on GluA1i alone or GluA1i + CNIH-2 (another AMPA-receptor-associated protein)[12,13] or GluA1i + γ-5 (**Fig. 2a**, **Supplementary Fig. 1** and **Supplementary Table 1a**). Perampanel blocked AMPA receptors independently of TARPs, as did GYKI53784 (**Supplementary Fig. 2** and **Supplementary Table 1b,c**). LY3130481 potently and efficaciously blocked all of the γ-8-containing homomeric AMPA receptors that displayed measurable steady-state glutamate-evoked currents (GluA1i, GluA2i, GluA3i, GluA4i and GluA1o), indicating that the γ-8-specific antagonistic actions were not GluA subunit dependent (**Fig. 2a–e**, **Supplementary Fig. 3** and **Supplementary Table 1a**). GluA2o, GluA3o and GluA4o homomers did not show measurable currents. LY3130481 also antagonized γ-8-containing GluA1/2 heteromers, the primary AMPA receptor in hippocampal neurons[14]. CNIH-2 and CNIH-3 have crucial roles in native hippocampal AMPA receptors[15], and LY3130481 potently blocked GluA1/2 heteromers containing γ-8 + CNIH-2, whereas it only minimally antagonized CNIH-2-containing AMPA receptors with either γ-2 or γ-4 (**Fig. 2f**, **Supplementary Fig. 4** and **Supplementary Table 1a**). Given that CNIH-2 reduces γ-8 stoichiometry of AMPA receptors[16], we wondered whether the partial inhibition was explained by the presence of fewer γ-8 molecules per AMPA receptor. We therefore reduced γ-8 stoichiometry using a GluA1i/γ-8 tandem construct that we co-transfected with GluA1i or GluA2i[13,16]. Indeed, LY3130481 was less efficacious and slightly less potent against AMPA receptors with lower γ-8 stoichiometry, as compared to GluA1i/γ-8 (**Fig. 2g**, **Supplementary Fig. 4a–f** and **Supplementary Table 1a**). LY3130481 antagonized GluA2i + γ-8 less efficaciously than the other γ-8-containing AMPA receptors (**Fig. 2b**). This difference was probably not a result of lower γ-8 stoichiometry to GluA2i, but rather of the intrinsic properties of GluA2i + γ-8 (**Supplementary Fig. 4a,g–i**). LY3130481 antagonism showed no strong cooperativity (**Supplementary Table 1a**) and was not competitive with glutamate (**Fig. 2h** and **Supplementary Table 1d**).

Domain swapping and mutational studies between γ-8 and γ-4 revealed that two amino acids (valine 177 and glycine 210 in transmembrane domains 3 and 4, respectively) close to the extracellular milieu were crucial for the selectivity of LY3130481 (**Fig. 2i,j**, **Supplementary Figs. 5–7** and **Supplementary Table 1e**). Given that these two amino acids are unique to γ-8 and are not present in other type I TARPs (**Supplementary Fig. 6f**), we generated the corresponding γ-2 point mutants. Consistently with the γ-4 mutants, double amino acid substitution in γ-2 conferred high sensitivity to LY3130481, and the single amino acid substitutions yielded moderate sensitivity to LY3130481 (**Fig. 2k**, **Supplementary Fig. 8** and **Supplementary Table 1e**).

LY3130481 antagonized AMPA receptors in hippocampal or cerebrocortical neurons, but not cerebellar Purkinje neurons (**Fig. 3a**, **Supplementary Fig. 9a** and **Supplementary Table 1f**). The partial inhibition profile of LY3130481 in neurons was comparable to that observed in recombinant AMPA receptors with reduced γ-8 stoichiometry, that is, CNIH-2-containing or GluA1i/γ-8 tandem + GluA1 or 2 (**Fig. 2f,g** and **Supplementary Table 1a**). Notably, LY3130481 had no effect on hippocampal neurons from γ-$8^{-/-}$ (*Cacng8*$^{-/-}$) mice (**Fig. 3b** and **Supplementary Fig. 9b**). By contrast, perampanel did not show brain-region specificity for AMPA-receptor inhibition (**Supplementary Fig. 9c** and **Supplementary Table 1f**)[4].

LY3130481 also antagonized excitatory synaptic transmission. In rat or mouse hippocampal slices, LY3130481 gradually and significantly blocked field excitatory postsynaptic potentials (fEPSPs) at Schaffer-collateral-CA1 synapses (**Fig. 3c–f**), whereas it had no effect in γ-$8^{-/-}$ mice (**Fig. 3c,d**). The slow onset of fEPSP blockage by

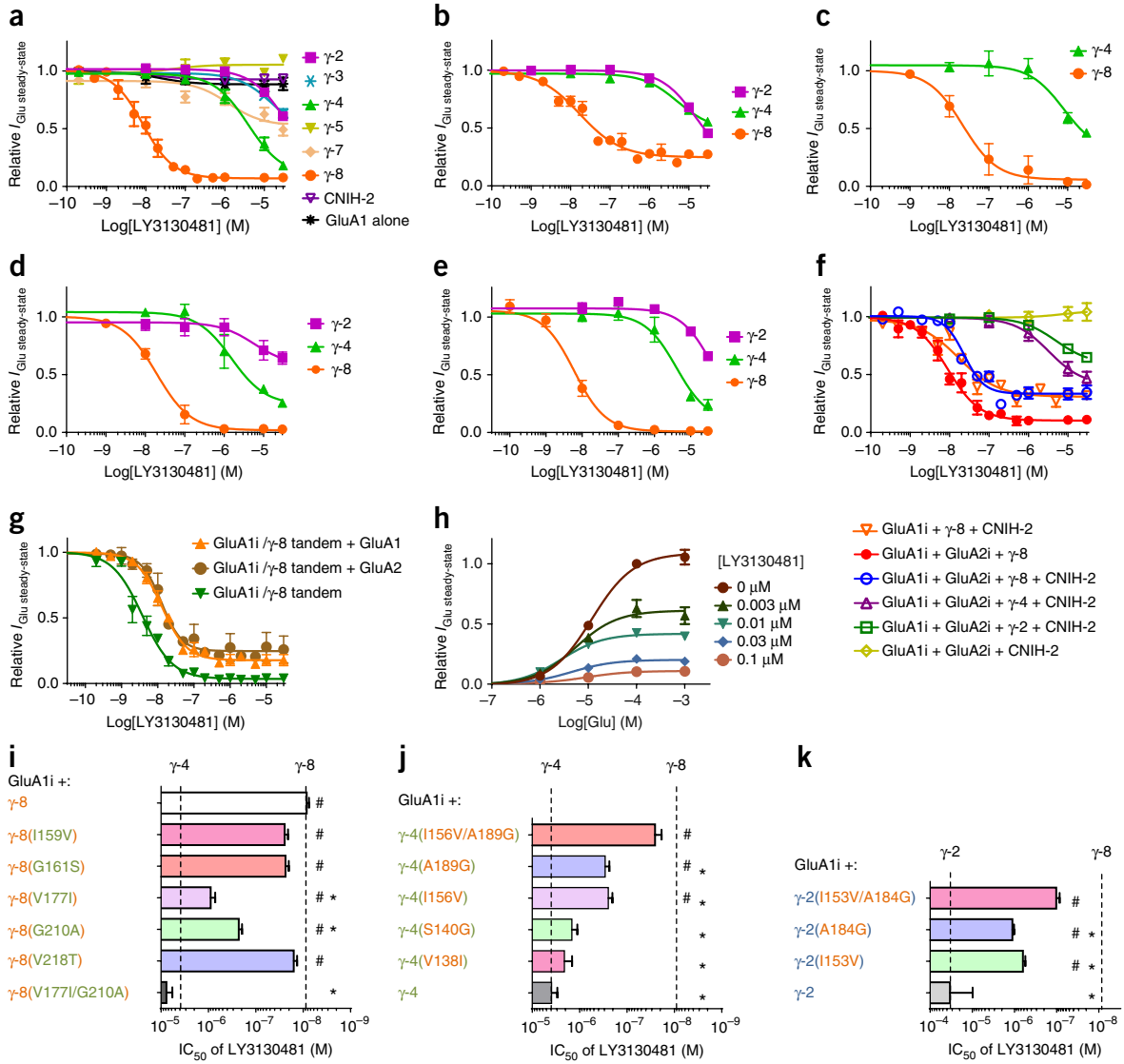

Figure 2 LY3130481 potently and selectively blocks all AMPA-receptor complexes that contain γ-8. (**a**–**f**) Concentration-response curves (CRCs) for the inhibition of glutamate-evoked currents by LY3130481 in HEK293T cells transfected with GluA1i (**a**), GluA2i (**b**), GluA3i (**c**), GluA4i (**d**), GluA1o (**e**), GluA1i + GluA2i heteromers (**f**) and auxiliary subunits, as indicated. Responses were evoked by 1 mM glutamate, and steady-state currents were measured. (**g**) The CRCs of LY3130481 for the AMPA receptors with coexpression of GluA1i or GluA2i with GluA1i/γ-8 tandem. AMPA receptors with GluA + γ-8 or GluA/γ-8 tandem had higher γ-8 stoichiometry than those with GluA + GluA1i/γ-8 tandem[13,16]. (**h**) Noncompetitive antagonism by LY3130481. Currents evoked by glutamate in the presence of various concentrations of LY3130481. Data points and error bars represent mean ± s.e.m. The numbers of the recorded transfectants and IC_{50} are shown in **Supplementary Table 1a**,**d**. (**i**,**j**) Identification of two amino acids crucial for the selectivity of LY3130481. IC_{50} of LY3130481 for the glutamate-evoked currents from GluA1i + γ-8 (**i**) or γ-4 (**j**) point mutants. Domain swapping between γ-8 and γ-4 identifying the unique amino-acids for γ-8 are shown in **Supplementary Figures 5**–**7**. The numbers of the recorded transfectants and IC_{50} are shown in **Supplementary Table 1e**. Vertical dotted lines highlight the IC_{50} values of γ-4 and γ-8. Error bars indicate s.e.m. $^{*}P < 0.001$ compared with GluA1 + γ-8, $^{\#}P < 0.001$ compared with GluA1 + γ-4 with Dunnett's test. (**k**) Potency of LY3130481 in γ-2 mutants substituted with amino acids from γ-8. Vertical dotted lines highlight the IC_{50} values of γ-2 and γ-8. $^{*}P < 0.001$ compared with GluA1 + γ-2(I153V/A184G); $^{\#}P < 0.001$ compared with GluA1 + γ-2 with Dunnett's test.

LY3130481 in hippocampal slices (**Fig. 3d**,**e**) is probably a result of slow LY3130481 penetration into the slices (**Supplementary Fig. 10**). Radio-ligand displacement experiments to assess the binding selectivity of LY3130481 to other neurotransmitter receptors, ion channels and transporters revealed that LY3130481 did not exhibit substantial (>40%) modulation of radioligand binding (**Supplementary Table 2**), and FLIPR assays revealed that LY3130481 did not functionally modulate kainate, NMDA or metabotropic glutamate receptors (**Supplementary Table 3a**,**b**). To assess LY3130481 effects *in vivo*, we counted the spikes evoked by either iontophoretically applied AMPA or NMDA in CA1 hippocampal regions of anesthetized rats. Both AMPA and NMDA evoked robust and transient spikes. Systemically administered LY3130481 reduced AMPA-evoked, but not NMDA-evoked, activities in a dose-dependent manner (**Fig. 3g**,**h**). Notably, AMPA-evoked spiking activity was not antagonized in the rat red nucleus, a brain area, similar to cerebellum, with a very low density of TARP γ-8 (**Supplementary Fig. 11**). The molecular mechanisms underlying the blockage of γ-8-containing AMPA receptors

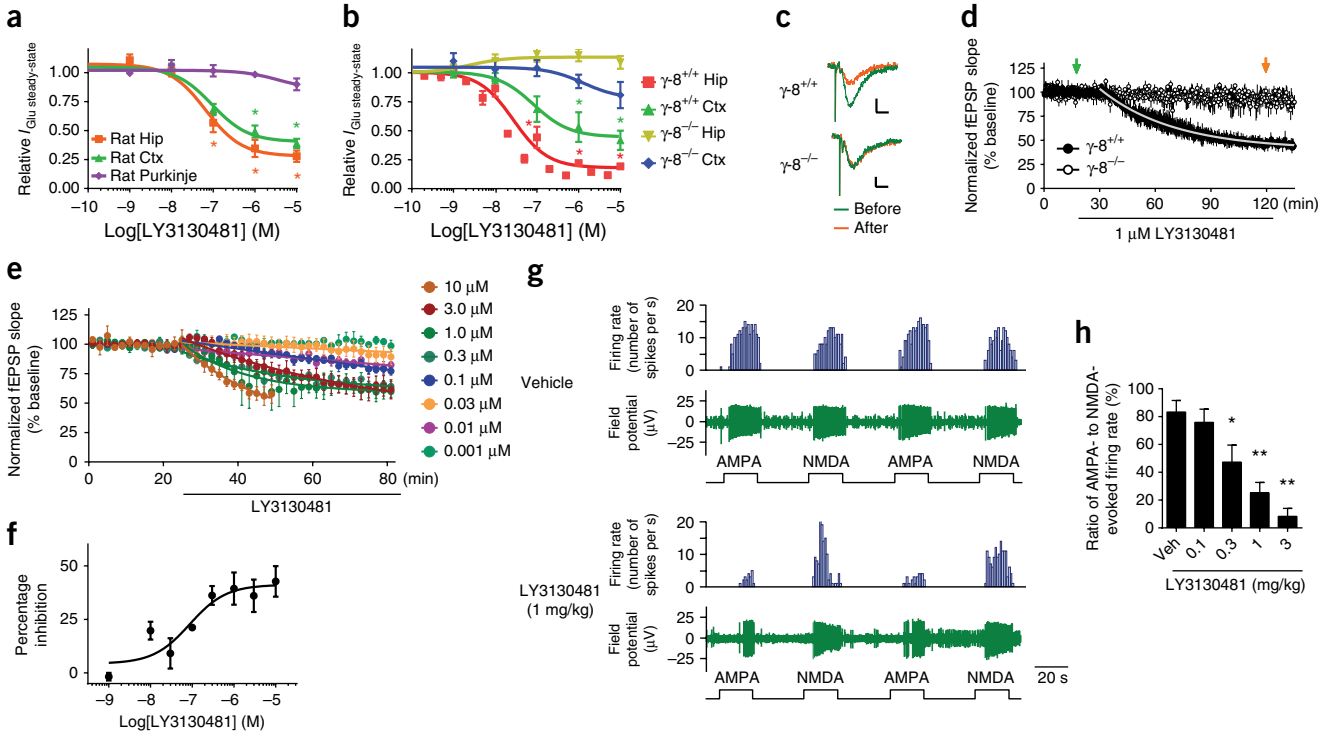

Figure 3 LY3130481 potently and partially blocks native γ-8-containing, but not γ-8-lacking, AMPA receptors. (**a**) CRCs for inhibition of glutamate-evoked (1 mM) currents by LY3130481 on acutely isolated rat hippocampal, cortical or cerebellar Purkinje neurons. $*P < 0.001$ compared with the cerebellar neurons using Tukey's test. (**b**) The CRCs of LY3130481 on acutely isolated the hippocampal and cortical neurons from γ-$8^{+/+}$ or γ-$8^{-/-}$ mice. Error bars indicate s.e.m. The number of the recorded transfectants and IC_{50} are in **Supplementary Table 1f**. $*,^{\#}P < 0.001$ compared with the hippocampal (*) or cortical neurons (#) from γ-$8^{-/-}$ using Tukey's test. (**c**,**d**) γ-8-dependent blockage of fEPSP at hippocampal Schaffer-CA1 synaptic transmissions by LY3130481. (**c**) Typical traces before (green) and after (orange) the application of LY3130481. Scale bars represent 10 ms, 0.1 mV. (**d**) Change in the slopes of the first fEPSP is plotted as a function of time (number of recordings: γ-$8^{+/+}$, $n = 4$; γ-$8^{-/-}$, $n = 3$). The time constant of fEPSP slope change in γ-$8^{+/+}$ slices by LY3130481 was calculated by fitting with single-phase decay curve ($\tau_{1\ \mu M} = 40$ min). Data points and error bars represent mean ± s.e.m. (**e**) Concentration-dependent reductions in the fEPSP slopes of rat Schaffer-CA1 synapses at various concentrations of LY3130481 (time constant of change in fEPSP slopes: $\tau_{0.3\ \mu M} = 30$ min, $\tau_{1.0\ \mu M} = 17$ min, $\tau_{3.0\ \mu M} = 54$ min, $\tau_{10\ \mu M} = 22$ min). Data points and error bars represent mean ± s.e.m. (**f**) CRC of the LY3130481 for the rat hippocampal neurotransmission (mean ± s.e.m., $IC_{50} = 87.5$ nM). (**g**) Field potential recordings evoked by iontophoretically administered AMPA or NMDA at the CA1 area of anesthetized rats with systemic injection of LY3130481 at different doses. The field potential and the firing rate (spike number per s) are shown with green traces and blue bar graphs, respectively. (**h**) Dose dependence of LY3130481 on the ratio of the AMPA- to NMDA-evoked firing rate. Data points and error bars represent mean ± s.e.m. (number of recordings: Veh, $n = 8$; 0.1, $n = 5$; 0.3, $n = 7$; 1.0, $n = 7$; 3.0, $n = 6$). $**P < 0.001$, $*P < 0.05$, as compared with vehicle control using Dunnett's test.

by LY3130481 are unclear. Pharmacological and biochemical analyses suggested that LY3130481 probably does not involve dissociation of γ-8 from AMPA receptors (**Supplementary Fig. 12**).

Oral administration of LY3130481 potently and dose-dependently suppressed the clonic convulsions induced by pentylenetrazole (PTZ) in rats ($ED_{50} = 1.7$ mg/kg) (**Fig. 4a**). No motor deficits were observed at doses up to 100 mg/kg (**Fig. 4b**). By contrast, GYKI52466 and perampanel acted as anticonvulsants (**Fig. 4a**) only at doses that produced marked motor impairment (**Fig. 4b**). LY3130481 and perampanel also acted as anticonvulsants in rats that were fully sensitized to repeated daily exposure to electrically induced seizures (kindling) via the basolateral amygdala in comparison with the antiepileptic valproate (**Fig. 4c**). Notably, and in contrast with perampanel, LY3130481 produced small increases in locomotion, consistent with γ-$8^{-/-}$ mice showing hyperlocomotion[17] (**Fig. 4d**). The anticonvulsant effects of LY3130481 were abolished in γ-$8^{-/-}$ mice, whereas the anticonvulsant effects of GYKI52466 and perampanel remained (**Fig. 4e**). Perampanel (1 and 2 mg/kg) induced tremor, ataxia, running, bouncing and tonic-clonic forelimb seizures with falling in mice with kainate-induced mesial temporal lobe epilepsy, effects that have not been observed in non-epileptic mice[18]. Thus, we conducted two experiments to evaluate the effects of LY3130481 on mice with epilepsy. Mice with kainate-induced mesial temporal lobe epilepsy exhibited 16.3 ± 1.3 spontaneous recurrent hippocampal paroxysmal discharges, and these were completely eliminated by 15 min after treatment with LY3130481 (6 mg/kg, i.p). In mice kindled with PTZ (45 mg/kg, subcutaneous, every other day) for 5 d, the percentage of mice exhibiting clonus was 83.0 ± 7.3 ($n = 24$) on day 8. Both LY3130481 (10 mg/kg, intraperitoneal (i.p.)) and perampanel (30 mg/kg, i.p.) significantly reduced the prevalence of kindled seizures (**Fig. 4f**). However, perampanel, but not LY3130481, caused motor impairment in naive and PTZ-kindled mice (**Fig. 4f**). LY3130481 also engendered a qualitatively different motor signature in mice than perampanel, with increases in ambulations and vertical movements, whereas perampanel decreased these behaviors (**Fig. 4g**). We next reconstituted AMPA receptors from hippocampal tissue obtained from a patient with epilepsy into *Xenopus* oocytes[4]. These AMPA-receptor currents were dose-dependently attenuated by LY3130481 (**Fig. 4h**,**i**), whereas comparable AMPA currents from the human cerebellum were not (**Fig. 4j**). Perampanel blocks AMPA currents in both cortex and cerebellum[4].

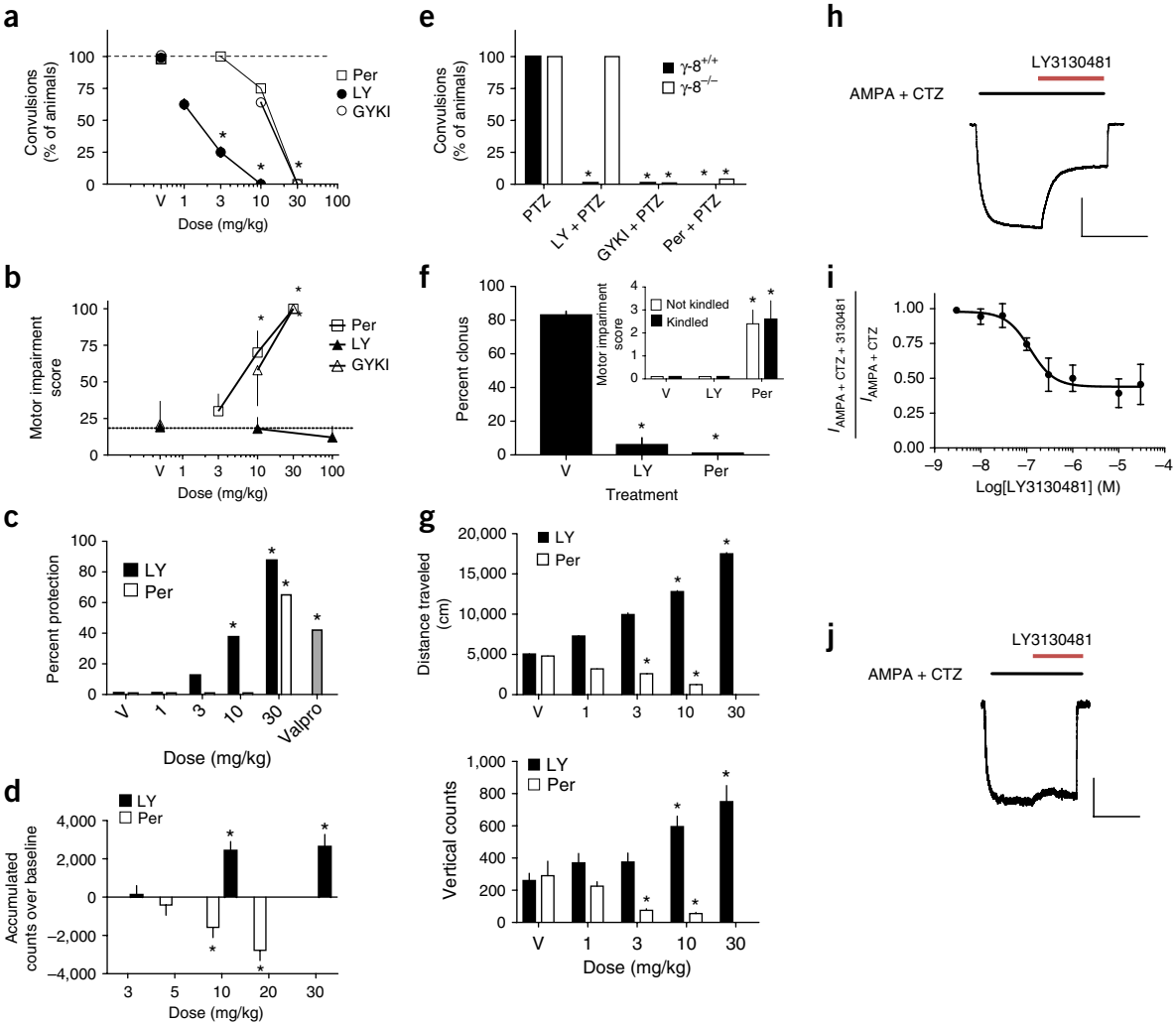

Figure 4 Anticonvulsant effects of LY3130481, on motor performance and on excitatory currents from AMPA receptors expressed in human hippocampal epileptic tissue. (**a**) Percentage of animals with convulsions induced by pentylenetetrazole as a function of dose of LY3130481 (*per os*, p.o.), GYKI52466 (i.p.) or perampanel (i.p.). (**b**) Motor impairment as a function of drug administration (LY3130481 (LY), perampanel (Per) and GYKI52466 (GYKI)). (**c**) Effects of LY3130481 on fully expressed basolateral amygdala kindled seizures induced by 400 μA ($F = 21.4$, $P < 0.0001$, $n = 8$/group; $ED_{50} = 16.4$ (8.2–29) mg/kg). $^*P < 0.05$, Fisher's exact test compared with vehicle control value. V, vehicle; effects of valproic acid (Valpro: (300 mg/kg, i.p.) are shown as a positive control). $^*P < 0.05$, Fisher's exact test, $n = 5$ rats/group. (**d**) Effects of LY3130481 on locomotor activity of rats in comparison with perampanel. $^*P < 0.05$, ANOVA followed by *post hoc* Dunnett's test. (**e**) Comparative effects of LY3130481 (10 mg/kg), GYKI52466 (30 mg/kg, i.p.) and perampanel (30 mg/kg, i.p.) in γ-$8^{-/-}$ and γ-$8^{+/+}$ mice against PTZ-induced seizures. $^*P < 0.05$, Fisher's exact probability test compared with PTZ alone. (**f**) Seizure and motor ratings (inset) in the presence or absence of LY3130481 (10 mg/kg, i.p.) or perampanel (30 mg/kg, i.p.) for the mice that were seizure kindled by every other day dosing with PTZ. $^*P < 0.05$, Fisher's exact probability test compared with control (V). (**g**) Effects of LY3130481 versus perampanel on locomotion of mice assessed by distance traveled (top) and instances of vertically directed behaviors such as rearing (bottom.). $^*P < 0.05$, ANOVA followed by *post hoc* Dunnett's test compared with vehicle control (V). (**h**) Representative trace of currents evoked by AMPA + cyclothiazide (CTZ) from *Xenopus* oocyte membranes micro-implanted with human epileptic hippocampal tissue. LY3130481 (10 μM) was co-applied 5 min after the application of AMPA (100 μM) + CTZ (30 μM). Scale bars represent 5 min and 50 nA. (**i**) The relative amplitude of steady-state AMPA + CTZ-evoked currents in the presence of LY3130481 recorded from *Xenopus* oocytes with human hippocampal membrane fraction was plotted as a function of LY3130481 concentration. Data are presented as means ± s.e.m. of three independent experiments. IC_{50}, 114 nM. (**j**) A representative trace from the oocyte procedures except using human cerebellar membranes for micro-implantation instead of hippocampus as in **i**. Scale bars represent 5 min and 20 nA.

Our results illustrate the engineering of a selective modulator of forebrain function on the basis of a specific auxiliary protein for a receptor regulating fast synaptic transmission. Although there are medicines that interact with auxiliary subunits of other ion channels (for example, gabapentin for the α2δ subunit of voltage-gated calcium channels and sulfonylurea drugs for the SUR subunit of K_{ATP} channels), neither these drugs nor their mechanisms of action were rationally designed or directed toward regional circuits. Several neurotransmitter receptors contain auxiliary subunits[5,19]. Screening of compounds that selectively target auxiliary proteins as we did will enable the identification of chemicals that selectively modulate brain areas involved in disease while minimizing side effects. Given that neuronal receptors can associate with a range of auxiliary proteins that have differential localization and functional controls over specific neural circuits, our strategy has far-reaching consequences.

METHODS

Methods and any associated references are available in the online version of the paper.

Note: Any Supplementary Information and Source Data files are available in the online version of the paper.

ACKNOWLEDGMENTS

We are grateful to the US National Institutes of Health Anticonvulsant Screening Program of the US National Institutes of Neurological Disorders and Stroke, National Institutes of Health (http://www.ninds.nih.gov/research/asp/), for their help with the mesial temporal lobe assessments. In particular, we are grateful for the expert support of T. Chen, S. Raeissi and program director J. Kehne and to their associated laboratories at the University of Utah, directed by H.S. White. We also thank Covance Laboratories, particularly D. Modlin, for their assistance with the amygdala kindling studies, and M.W. Jeffries (Eli Lilly) for transfection. While this manuscript was under review, the following manuscripts were published: Gardinier *et al.*, 2016 (ref. 9), describing the synthesis of LY3130481; Maher *et al.*, 2016 (ref. 20), describing an alternative molecule with TARP γ-8 selectivity and anticonvulsant activity; and Witkin and Gardinier, 2016 (ref. 21), detailing discovery and disclosure dates for LY3130481 as the first TARP-dependent antagonist. On 26 September 2016, Cerecor Inc. announced the acquisition of LY3130481 (now CERC-611) from Eli Lilly and Company for development in patients with epilepsy.

AUTHOR CONTRIBUTIONS

J.M.W. designed the anticonvulsant and behavioral experiments and interpreted the associated data, wrote the manuscript and served as the biological leader of the project. A.S.K. designed, performed and interpreted the data from most of the electrophysiological and biochemical experiments, and wrote the manuscript. K.D.B., C.D., Y.T., D.A.S. and H.Y. designed, performed and interpreted the data from the FLIPR screening experiments. K.M.G. (chemistry leader), D.L.G., W.J.P., J.R., B.A.H. and P.L.O. performed chemical design and synthesis of LY3130481. F.P. and S.M.F. contributed electrophysiological recordings from hippocampal slices. R.Z. and E.S. designed and performed the *Xenopus* oocyte experiment. Y.Q., H.W. and M.R.L. designed and constructed the TARP mutant cDNAs. T.E.F. and K.R. designed and performed *in vivo* electrophysiological recordings. S.D.G. and K.A.W. designed and conducted anticonvulsant and behavioral studies. J.T.C. planned and executed experiments on tissue permeability. J.T.R.I. and E.S.N. designed electrophysiological experiments and provided expert advice. D.S.B. initiated the project with the key concept of this study.

COMPETING FINANCIAL INTERESTS

The authors declare competing financial interests: details are available in the online version of the paper.

1. Huganir, R.L. & Nicoll, R.A. AMPARs and synaptic plasticity: the last 25 years. *Neuron* **80**, 704–717 (2013).
2. Hibi, S. *et al.* Discovery of 2-(2-oxo-1-phenyl-5-pyridin-2-yl-1,2-dihydropyridin-3-yl)benzonitrile (perampanel): a novel, noncompetitive α-amino-3-hydroxy-5-methyl-4-isoxazolepropanoic acid (AMPA) receptor antagonist. *J. Med. Chem.* **55**, 10584–10600 (2012).
3. French, J.A. *et al.* Adjunctive perampanel for refractory partial-onset seizures: randomized phase III study 304. *Neurology* **79**, 589–596 (2012).
4. Zwart, R. *et al.* Perampanel, an antagonist of α-amino-3-hydroxy-5-methyl-4-isoxazolepropionic acid receptors, for the treatment of epilepsy: studies in human epileptic brain and nonepileptic brain and in rodent models. *J. Pharmacol. Exp. Ther.* **351**, 124–133 (2014).
5. Jackson, A.C. & Nicoll, R.A. The expanding social network of ionotropic glutamate receptors: TARPs and other transmembrane auxiliary subunits. *Neuron* **70**, 178–199 (2011).
6. Partin, K.M., Patneau, D.K., Winters, C.A., Mayer, M.L. & Buonanno, A. Selective modulation of desensitization at AMPA versus kainate receptors by cyclothiazide and concanavalin A. *Neuron* **11**, 1069–1082 (1993).
7. Turetsky, D., Garringer, E. & Patneau, D.K. Stargazin modulates native AMPA receptor functional properties by two distinct mechanisms. *J. Neurosci.* **25**, 7438–7448 (2005).
8. Tomita, S. *et al.* Stargazin modulates AMPA receptor gating and trafficking by distinct domains. *Nature* **435**, 1052–1058 (2005).
9. Gardinier, K.M. *et al.* Discovery of the first α-amino-3-hydroxy-5-methyl-4-isoxazolepropionic acid (AMPA) receptor antagonist dependent upon transmembrane AMPA receptor regulatory protein (TARP) γ-8. *J. Med. Chem.* **59**, 4753–4768 (2016).
10. Cokić, B. & Stein, V. Stargazin modulates AMPA receptor antagonism. *Neuropharmacology* **54**, 1062–1070 (2008).
11. Kott, S., Werner, M., Körber, C. & Hollmann, M. Electrophysiological properties of AMPA receptors are differentially modulated depending on the associated member of the TARP family. *J. Neurosci.* **27**, 3780–3789 (2007).
12. Schwenk, J. *et al.* Functional proteomics identify cornichon proteins as auxiliary subunits of AMPA receptors. *Science* **323**, 1313–1319 (2009).
13. Shi, Y. *et al.* Functional comparison of the effects of TARPs and cornichons on AMPA receptor trafficking and gating. *Proc. Natl. Acad. Sci. USA* **107**, 16315–16319 (2010).
14. Geiger, J.R. *et al.* Relative abundance of subunit mRNAs determines gating and Ca^{2+} permeability of AMPA receptors in principal neurons and interneurons in rat CNS. *Neuron* **15**, 193–204 (1995).
15. Kato, A.S. *et al.* Hippocampal AMPA receptor gating controlled by both TARP and cornichon proteins. *Neuron* **68**, 1082–1096 (2010).
16. Gill, M.B. *et al.* Cornichon-2 modulates AMPA receptor-transmembrane AMPA receptor regulatory protein assembly to dictate gating and pharmacology. *J. Neurosci.* **31**, 6928–6938 (2011).
17. Gleason, S.D. *et al.* Inquiries into the biological significance of transmembrane AMPA receptor regulatory protein (TARP) γ-8 through investigations of TARP γ-8 null mice. *CNS Neurol. Disord. Drug Targets* **14**, 612–626 (2015).
18. Twele, F., Bankstahl, M., Klein, S., Römermann, K. & Löscher, W. The AMPA receptor antagonist NBQX exerts anti-seizure but not antiepileptogenic effects in the intrahippocampal kainate mouse model of mesial temporal lobe epilepsy. *Neuropharmacology* **95**, 234–242 (2015).
19. Tomita, S. & Castillo, P.E. Neto1 and Neto2: auxiliary subunits that determine key properties of native kainate receptors. *J. Physiol. (Lond.)* **590**, 2217–2223 (2012).
20. Maher, M.P. *et al.* Discovery and characterization of AMPA receptor modulators selective for TARP-γ8. *J. Pharmacol. Exp. Ther.* **357**, 394–414 (2016).
21. Witkin, J.M. & Gardinier, K.M. A comment on "Discovery and characterization of AMPA receptor modulators selective for TARP-γ8". *J. Pharmacol. Exp. Ther.* **358**, 502–503 (2016).

ONLINE METHODS

FLIPR screening. Inhibition of glutamate-stimulated activation of AMPA receptors was determined in CHO-S cells (Invitrogen) that transiently express human GluA1 and TARPs. For GluA1-γ-8 transfection, we constructed the plasmids expressing human GluA1o and human γ-8 bi-cistronically using pBudCE4.1 vector (Thermo Fisher), and co-transfected it into CHO-S cells with human EAAT3 cDNA at a ratio of 2:3. For GluA1-γ-2 transfection of CHO-S cells, bi-cistronically expressing human GluA1o-and human γ-2 inserted in pBudCE4.1 (Thermo Fisher) was used. For the TARP-less AMPA receptors, we used human GluA1-flip (GluA1i) in pcDNA3.1 (Thermo Fisher). Due to the relatively small dynamic range of calcium dyes, we needed to make the FLIPR signals comparable between the AMPA receptors with and without TARPs. To solve the issue, we used flip and flop isoform for TARP-less and TARP-containing transfectants, respectively. Flip isoforms have greater conductance than flop isoforms[22], and TARPs enhance AMPA receptor functions of both flip and flop isoforms[5]. Parental CHO-S cells were grown in suspension in 50/50 custom media to a density of 10^7 cells/ml. 50/50 is a 1:1 (v/v) mixture of CD CHO (Gibco #10743) and a custom complete media. The custom complete media was made by adding 0.40 mg/l tropolone, 5.00 mg/l insulin, 20 mM HEPES and 0.075% Pluronic F68 to a custom basal media having the following formula: (values as mg/l unless otherwise specified) 11.01 anhydrous calcium chloride, 0.050 ferric nitrate-9H_2O, 0.420 ferrous sulfate-7H_2O, 28.64 anhydrous magnesium chloride, 48.84 anhydrous magnesium sulfate, 312.14 KCl, 5505.96 NaCl, 62.57 monobasic sodium phosphate, 71.28 anhydrous dibasic sodium phosphate, 0.432 zinc sulfate-7H_2O, 10.0 ethanolamine HCl, 6000 D-glucose (dextrose), 0.210 DL lipoic acid thioctic, 0.081 putrescine 2 HCl, 4.78 sodium hypoxanthine, 220.24 sodium pyruvate, 0.730 thymidine, 8.90 L-alanine, 211.23 L-arginine HCl, 15.02 L-asparagine H_2O, 13.31 L-aspartic acid, 62.67 cystine 2 HCl, 7.360 L-glutamic acid, 146.16 l-glutamine, 30.0 glycine, 42.04L-histidine HCl 2 H_2O, 105.11 L-isoleucine, 105.11 L-leucine, 146.16 L-lysine HCl, 30.03 L-methionine, 66.07 L-phenylalanine, 17.27 L-proline, 42.04 L-serine, 95.1 L-threonine, 16.02 L-tryptophan, 104.11 l-tyrosine disodium salt, 94.1 L-valine, 8.99 choline chloride, 4.00 folic acid, 12.61 inositol, 4.00 niacinamide, 4.00 pyridoxal HCl, 0.031 pyridoxine HCl, 0.400 riboflavin, 4.00 sodium pantothenate, 4.00 thiamine HCl, 0.680 vitamin B12, and 2200 sodium bicarbonate. Cells were centrifuged at 1,000*g* for 15 min and resuspended in fresh 50/50 custom media at 2×10^6 cells/ml. For batch transfection, 2 mg of total DNA(s) was used for each liter of cells. DNA(s) and FreeStyleMAX (Thermo Fisher cat#16447-500) were added to basal custom media (see above) in the proportions of 10 μg total DNA: 10 μl FreeStyleMAX: 1 ml media, to form a DNA complex. After 15 min, an appropriate volume (20% v/v) of DNA complex was added to the prepared cell culture. Transiently transfected CHO-S cells were harvested after 48 h and frozen in aliquots for later use. The function and pharmacology of AMPA receptors in transfected cells was verified in both freshly prepared and thawed aliquots of cells. Frozen transfected CHO-S cells expressing AMPA receptors were thawed and plated in Dulbecco's Modified Eagle's Medium (DMEM media) (Thermo Fisher, cat.# 11960) containing 5% dialyzed fetal bovine serum (Thermo Fisher, cat.# 26400-036) and 20 mM HEPES at 50,000 cells per well in 384-well Poly-D-lysine coated plates (Becton Dickinson, cat.#354663) and cultured overnight at 37 °C. On the day of an experiment, two fluorescence dye loading buffers were prepared. Fluo-4-a.m. dye loading buffer consists of 5 μM Fluo-4 a.m. dye (Molecular Probes, cat# F-14202) in Hank's Balanced Salt Solution (HBSS) containing 20 mM HEPES (pH 7.4), 2.5 mM probenecid (Sigma-Aldrich, cat.# P8761) and 5 nM Pluronic F-127 (Molecular Probes, cat.# P3000MP). Fluo-4 NW dye loading buffer was prepared by adding 100 ml of HBSS containing 20 mM HEPES (pH 7.4) and 2.5 mM probenecid to one bottle of Fluo-4 NW dye (Molecular Probes, high throughput pack, cat# F36205). Cultured GluA1-γ-8 and GluA1-γ-2 CHO-S cells were loaded with Fluo-4 a.m. dye loading buffer and incubated at 22 °C for 2 h. GluA1flip CHO-S cells were loaded with Fluo-4 NW dye loading buffer and incubated at 37 °C for 30 min followed by incubation for 90 min at 22 °C. Following incubations, the dye loading buffer in the cell plate was removed, and fresh assay buffer was added. Assay buffer consisted of HBSS with 20 mM HEPES (pH 7.4), 2.5 mM probenecid and 4 mM $CaCl_2$. The assay was initiated by the addition of compounds, followed 2 min later by addition of glutamate (5 μM final). 2 min later, cyclothiazide (20 μM final) and glutamate (45 μM final) were added. Changes in intracellular [Ca^{2+}] were kinetically recorded by a fluorescence-imaging plate reader (FLIPR). Inhibition of the effect of glutamate by test compounds was expressed as a percentage of the responses stimulated by glutamate plus CTZ in the presence of test compounds relative to the maximum inhibition defined by using 167 μM GYKI53784, a nonselective AMPA antagonist, and the baseline defined by assay buffer alone. The actions of LY3130481 on kainate receptors were evaluated using the HEK293 cells (ATCC) stably expressing human GluK2Q. The Fluo-4-a.m. loaded cells were pre-incubated with 250 μg/ml concanavalin A for 30 min. To evaluate the antagonistic action of LY3130481, we added various concentrations of LY3130481, and then added 100 μM glutamate. The effect of LY3130481 on NMDA receptors was tested using HEK293 cells with human GluN1/GluN2A or GluN1/GluN2B cDNA under the control of TET-on operator with CMV promotor. The expression of NMDA receptors was induced by 1 μg/ml doxycycline. To evaluate possible potentiator action, we added various concentrations of LY3130481 and then 0.2 μM glutamate + 2.5 μM glycine. Possible antagonistic activity was evaluated by the addition of LY3130481 and then 2 μM glutamate + 2.5 μM glycine. To evaluate the effects of LY3130481 on metabotropic glutamate receptors, we used AV12 cells (ATCC) stably expressing either of mGluR1, 2, 3, 4, 5 or 8 with EAAT1. To translate the activation of Gi-coupled mGluRs, mGluR2, 3, 4 and 8, to calcium mobilization, we co-expressed with a promiscuous G-alpha protein, Gα15. The cells were loaded with a calcium indicator, Fluo-3-a.m., Fluo-4-a.m. or Calcium-5 (Molecular Devices), and measured the change in the fluorescence intensity by the additions of 12.5–25 μM of LY3130481 and then glutamate. We used EC_{10} and EC_{90} concentrations of glutamate to assess possible potentiator and antagonist actions, respectively.

Chimeric cDNA constructions. The chimeric γ-8 and γ-4 constructs were engineered by PCR. The junctions of the transmembrane and extracellular/intracellular domains were predicted by a previous study[23] and our own sequence alignments. The regions of the designated domains are as follows (the number of amino acid residues): γ-8 (human Cacng8), TM1: 1-41, Ex1: 42-129, TM34: 158-228, C-term: 229-425, TM3: 158-179, Ex2: 180-205, TM4: 206-228. γ-4 (human Cacng4), TM1: 1-30, Ex1: 31-108, TM34: 137-207, C-term: 208-327, TM3: 137-158, Ex2: 159-184, TM4: 185-207. Point mutations were generated by PCR-based site-directed mutagenesis using custom oligonucleotides and Quikchange II (Agilent Technologies). GluA1/γ-8 construct was described previously[16].

Patch-clamp electrophysiology. Agonist-evoked currents were recorded from transfected HEK293T cells (ATCC) and acutely isolated neurons as described[24]. The rat neurons were isolated from 4–10 weeks old Sprague Dawley rats. The mouse neurons ranged from 4 to 10 weeks old CD-1 mice (γ-$8^{+/+}$) or γ-$8^{-/-}$ mice[25] that were backcrossed multiple times with CD-1 mice. We used both male and female animals. Kainate:glutamate ratios were calculated as $I_{KA\ steady\text{-}state}/I_{Glu\ steady\text{-}state}$, where $I_{KA\ steady\text{-}state}$ and $I_{Glu\ steady\text{-}state}$ are the steady-state responses evoked by kainate (1 mM) and glutamate (1 mM) application, respectively.

Resensitization percentage was calculated as $I_{Glu\ Resens}/\ I_{Glu\ steady\text{-}state} \times 100$, where $I_{Glu\ Resens}$ is the current that accrues from the trough of desensitization[15]. We discarded less than 5% of total recorded recombinant samples, which did not meet the criteria described in **Supplementary Figures 1–8**. We used all recordings from native neurons with stable and measurable steady-state currents. The potency of LY3130481 is calculated as follows. The amplitude of $I_{Glu\ steady\text{-}state}$ in the presence of LY3130481, normalized by that in the absence of LY3130481, was defined as relative to $I_{Glu\ steady\text{-}state}$, and plotted as a function of $\log_{10}$[LY3130481]. The average and s.e.m. of $\log_{10}IC_{50}$ and efficacy (I_{max}) are calculated using the pooled relative $I_{Glu\ steady\text{-}state}$ values recorded from three to 19 cells, as indicated in the figure legends, using three- or four-parameter sigmoidal curve fit with Prism 6.04 (GraphPad Software). We perfused 5–6 different concentrations of LY3130481 onto each cell. We put zero-drug values, that is, relative to $I_{Glu\ steady\text{-}state}$ without LY3130481 (= 1), at [LY3130481] = 1×10^{-13} M, which is three log units below the lowest LY3130481 concentration tested. We did not constrain either the bottom or top values for the curve-fitting

calculations, and so the calculated IC_{50} is relative to IC_{50}, which is the mid-point concentration between the top and bottom plateau. We calculated Hill co-efficient (nH) from curves containing more than 12 concentration points. The potency of glutamate is calculated as follows: we measured the $I_{Glu\ steady\text{-}state}$ without LY3130481 first, and then measured it under the perfusion of a fixed concentration of LY3130481, as indicated in **Figure 2g**. The $I_{Glu\ steady\text{-}state}$ in the presence of LY3130481 was normalized by the $I_{Glu\ steady\text{-}state}$ evoked by the initial 1 mM glutamate application without LY 3130481, and plotted as the function of log_{10}[Glu]. We used three-parameter sigmoidal curve fit and calculated the average and s.e.m. of $log_{10}IC_{50}$ and E_{max} using the pooled values of relative $I_{Glu\ steady\text{-}state}$ recorded from three cells for each concentration of LY3130481. We tested four glutamate concentrations for each cells. We put zero-glutamate values, that is, relative to $I_{Glu\ steady\text{-}state}$ without glutamate (= 0), at [Glu] = 1×10^{-8} M, which is two log units below the lowest glutamate concentration tested.

fEPSP recordings. fEPSPs were recorded from Schaffer-CA1 synapses of rats or mice. Parasagittal brain slices (400 µm) were prepared from 3–6-week-old animals using Vibroslice (Campden Instruments or Leica) in carbogenated (95% O_2 and 5% CO_2) ice-cold slicing solution (concentrations in mM): NaCl 124, $NaHCO_3$ 26, KCl 3, glucose 10, $CaCl_2$ 0.5, $MgCl_2$ 4 with 300–305 mOsm. The slices were incubated at 30–34 °C in carbogenated recording solution: NaCl 124, $NaHCO_3$ 26, KCl 3, glucose 10, $CaCl_2$ 2.3, $MgCl_2$ 1.3 with 300–305 mOsm for 30 min, and then allowed to rest at 20–25 °C for another 30 min before recording. Slices were then placed in a submersion-type recording chamber (RC-26G, Warner Instruments) mounted on an upright microscope (FN-1, Nikon) and continuously superfused (2–3 ml/min) with carbogenated recording solution. A concentric tungsten stimulation electrode and a recording electrode filled with 2 M NaCl were placed at stratum radiatum. Test pulses (100 µs pulse width) were applied every 20 s (0.05 Hz) or 30 s (0.067 Hz). Stimulation intensity was determined to obtain 50–70% of the maximum responses that elicit population spikes. The fEPSP slope after continuous LY3130481 perfusion (28 min for 10 µM or 60 min for the other concentrations) was normalized by the baseline, the mean fEPSP slope 20 min before LY3130481 perfusion, and the percentage of inhibition was calculated. We only used data with stable baselines. Concentration effect functions were generated, and these enabled construction of a concentration/% inhibition function with mean ± s.e.m. and the estimation of an IC_{50} value by three-parameter sigmoidal curve fitting methods within GraphPad Prism 6.04.

Iontophoretic application of AMPA and NMDA in rat hippocampus or red nucleus. Male Sprague Dawley rats (250–350 g) were anesthetized with 1.4 times body weight of 600 mg/ml urethane and implanted with a jugular cannula (PE 10 tubing attached to a 30-gauge needle) for intravenous (i.v.) drug administration. Animals were administered solutions of either LY3130481 (0.1, 0.3 or 1 mg/kg), GYKI53784 or vehicle (20% Captisol), intravenously. Cannulated animals were mounted on a rat stereotaxic frame, the skull was exposed, and a well opening was created, using a dental drill, at the following coordinates: AP −4.2, ML +2.4 for hippocampus, AP: −5.8 mm, ML: +0.8 to +1.1 mm for red nucleus. The dura was then cut, exposing the cortical surface. A five-barrel micropipette assembly mounted onto a Narishige micro-drive was lowered to a depth of DV: 1.8 mm to 2.6 mm for hippocampus or DV: 6.4 to 7.8 mm for red nucleus. The pipette barrels were pre-filled with solutions as follows: center recording barrel, 2 M NaCl; current balancing, 2 M NaCl; ejection vehicle, 190 mM NaCl, pH 8; AMPA, 1mM dissolved in the ejection vehicle; NMDA, 10 mM dissolved in the ejection vehicle. The pipette was slowly lowered to the target depth until a response from a CA1 pyramidal neuron or red nucleus neuron could be isolated and held. Signals were amplified by an XCell 3+ differential amplifier (Frederick Hauer). Low-frequency cut-off was set to 1,000 Hz, high-frequency cut-off was set to 2,000 Hz and gain was set to 20,000. Recordings of the cells' firing activity were made using Spike2 software. Alternating iontophoretic ejections of AMPA and NMDA were made using a Dagan 6400 programmable current generator. Ejections currents were titrated until stable levels of responding to pulses of AMPA and NMDA could be established, and then were held fixed. A baseline recording was then made, followed by recordings of the response to intravenous administration of vehicle or 0.1, 0.3 or 1 mg/kg of LY3130481. Data were analyzed using Spike2 software from CED. Cursor placement was used to demarcate AMPA and NMDA ejection pulses, and these cursor regions were analyzed for spike frequency across baseline, and post–drug administration epochs. Ratios of AMPA to NMDA mean firing rates (MFR) were then computed and averaged for each 5-min time interval postinjection, and expressed as percentage of baseline for each drug dose. Given that variances of percentage of baseline AMPA to NMDA ratios are not equal as they approach 0, data were log-transformed (log10) for further statistical analysis. Statistical evaluation of compound-treatment effects were made by one-way ANOVA for repeated measures. Transformed values for each 5-min effect mean, post injection, was treated as a repeated time measure. When significant *P* values from ANOVA were revealed, Dunnett's within-group dynamic multiple comparisons were evaluated to compare the effects of vehicle and drug-dose treatments.

Microtransplantation of brain membrane to *Xenopus* oocyte membranes. Frozen samples of human hippocampus and cerebellum were obtained from Oregon Brain Bank and Analytical Biological Services, respectively. The hippocampal sample was from a patient with epilepsy, and the cerebellar sample was from a control donor. Brain samples were kept frozen at −80 °C and transport of the samples from the USA to the UK took place on dry ice. Membrane preparations from these tissues were prepared according to the method developed and described[26–28]. In short: 0.1–0.5 g of tissue was homogenized in ice-cold glycine buffer (concentrations in mM: 200 glycine, 150 NaCl, 50 EGTA, 50 EDTA, 300 sucrose) to which 10 µl protease inhibitor cocktail (Sigma-Aldrich) was added per ml glycine buffer. The homogenate was centrifuged at 4 °C for 15 min at 9500*g*. The supernatant was subsequently centrifuged at 4 °C for 2 h at 100,000*g* with an ultra-centrifuge, and the pellet was re-suspended in ice-cold assay buffer (5 mM glycine). The protein concentration of the membrane preparations were measured using the Pierce BCA protein assay kit (Thermo Scientific) and were ~3 mg/ml. Aliquots of the suspensions were kept at −80 °C and were thawed just before injection into *Xenopus* oocytes. *Xenopus* oocytes (stage V–VI) were removed from schedule I sacrificed frogs and defolliculated after treatment with collagenase type I (5 mg/ml calcium-free Barth's solution) for 4 h at 20–23 °C. 60 nl of membrane suspension was injected per oocyte using a Drummond variable volume microinjector. After injection, oocytes were incubated at 18 °C in a modified Barth's solution containing (concentrations in mM): NaCl 88, KCl 1, $NaHCO_3$ 2.4, $Ca(NO_3)_2$ 0.3, $CaCl_2$ 0.41, $MgSO_4$ 0.82, HEPES 15 and 50 mg/l neomycin (pH 7.6 with NaOH; osmolarity 235 mOsm). Experiments used oocytes after 2–5 d of incubation. Oocytes were placed in a recording chamber (internal diameter 3 mm), which was continuously perfused with a saline solution (concentrations in mM): NaCl 115, KCl 2.5, $CaCl_2$ 1.8, $MgCl_2$ 1, HEPES 10, pH 7.3 with NaOH, 235 mOsm) at a rate of approximately 10 ml/min. Dilutions of drugs in external saline were prepared immediately before the experiments and applied by switching between control and drug-containing saline using a BPS-8 solution exchange system (ALA Scientific). Between responses, oocytes were washed for 2 min. Oocytes were impaled by two microelectrodes filled with 3 M KCl (0.5–2.5 MΩ) and voltage-clamped using a Geneclamp 500B amplifier (Axon Instruments). The external saline was clamped at ground potential by means of a virtual ground circuit using an Ag/AgCl reference electrode and a Pt/Ir current-passing electrode. The membrane potential was held at −60 mV. The current needed to keep the oocyte's membrane at the holding potential was measured. Membrane currents were low-pass filtered (four-pole low-pass Bessel filter, −3 dB at 10 Hz), digitized (50 Hz) and stored on disc for offline computer analysis. Data are expressed as mean ± s.e.m. Experiments were performed at 20–25 °C. For the inhibition curves, currents were evoked by switching to a solution containing 100 µM AMPA and 30 µM cyclothiazide (CTZ). After 5 min of AMPA/CTZ perfusion, the solution was switched to AMPA/CTZ plus various concentrations of LY3130481 for 5 min. Inhibition was calculated from the current amplitude at the end of LY3130481 application and the current amplitude of the AMPA/CTZ response just before LY3130481 application. The potency of LY3130481 is calculated as follows. The steady-state current amplitude evoked by AMPA + CTZ in the presence of LY3130481 was normalized by that in the absence of LY3130481 and was plotted as the function of Log[LY3130481]. We used three-parameter sigmoidal curve fit method in Prism 6 software to calculate the IC_{50}.

doi:10.1038/nm.4221

Selectivity assay by radioligand displacement. This assay was conducted by Cerep. The membrane fraction from rat brain or cells with heterologously expressed recombinant receptors was incubated with the radioligand shown in **Supplementary Table 2** in the presence or absence of 1 or 10 μM LY3130481 for 30–120 min at 4 °C, 22 °C or 37 °C. The binding reaction was terminated with rapid filtration, and the radioactivity retained on the filters was defined as total binding. Nonspecific binding was determined by including excess concentration of cold competitors shown in **Supplementary Table 2**. Specific binding was total binding subtracted by nonspecific binding. The percentage inhibition of specific binding by LY3130481 was calculated as: 100 − (specific binding in the presence of LY3130481/specific binding in the absence of LY3130481 × 100).

Measurement of LY3130481 concentration in hippocampal slices. Transverse hippocampal slices (400 μm thick) were prepared from 3–6-week-old Sprague Dawley rats and allowed to rest at 20–25 °C in carbogenated recording solution: NaCl 124, $NaHCO_3$ 26, KCl 3, glucose 10, $CaCl_2$ 2.3, $MgCl_2$ 1.3 with 300-305 mOsm for 30 min. The slices were transferred into a chamber with 1 μM LY3130481 in carbogenated recording solution. Ten slices (30–60 mg hippocampal tissue) were removed from LY3130481-containing solution, washed with ~50 ml of carbogenated recording solution three times and stored at −80 °C. The slices were homogenized in 300 μl of water/methanol (4:1, v/v). Stock solutions containing 1 mg/ml of LY3130481 were diluted to produce working solutions, which were then used to fortify control brain homogenate to produce calibration standards with concentrations ranging from 1 to 5,000 ng/ml. Aliquots of each study sample, calibration standard and control sample were then transferred to 96-well plates, mixed with acetonitrile/methanol (1:1, v/v) containing an internal standard to precipitate sample proteins, and centrifuged. The resulting supernatants were subjected to liquid chromatography with tandem mass-spectrometry analysis using an Applied Biosystems/MDS Sciex API 4000 equipped with a TurboIonSpray interface, operated in positive-ion mode. The analytes were chromatographically separated with a gradient-liquid-chromatography system and detected with selected reaction monitoring (M+H)+ transitions specific to LY3130481, *m/z* 383.1 > 232.1. The free fraction of LY3130481 was measured by placing LY3130481/brain mixture into one side of dialysis block and the buffer on the other side. After 4.5 h of incubation, the samples were taken from both sides. Fraction unbound is calculated by dividing the LC–MS/MS area of the buffer side by the LC–MS/MS area of the protein side.

General statistical considerations—*in vitro* data. Experiments with the FLIPR system were conducted blindly and with randomization. All other *in vitro* experiments were semi-randomized without blinding to condition. Group sizes were prospectively determined on the basis of previous publications assessing concentration response curves[29]. Decisions regarding statistical analyses were based on the nature of the data, distributions, homogeneity of variance and other statistically validated criteria. All data for ANOVA were evaluated for normally distributed functions, and the statistical analysis was handled accordingly, as noted. All data are provided with estimated variation, which is taken into account in statistical treatments. Specific cases are described in the figure legends and table captions. Data exclusion on occasion was determined a priori and statistically accepted outlier analyses as described in above.

Animal studies. Studies were performed according to the guidelines set forth by the National Institutes of Health and implemented by the Animal Care and Use Committee of Eli Lilly and Company and collaborative research institutes. All rodents used in this report were male. Group sizes were determined by a priori experience as appropriately powered to identify standard of care anticonvulsant and motor impairment. Animals were randomly assigned to treatment groups by independently drawing animals from their housing cages. For animal studies, the experimental observers were blinded to the treatments. In all studies, homogeneity of variances were assessed to determine the proper statistical treatment. For quantal data, no variances were created; data were replicated to assure the reliability of findings, as noted in figure legends.

PTZ-induced seizures. We administered LY3130481 (p.o.) or GYKI52466 (i.p.),or perampanel (i.p.) 30 min before subcutaneous PTZ (35 mg/kg) to evaluate their ability to prevent or dampen seizures induced in male Sprague Dawley rats (90–100 g, ~5 weeks old). After dosing, animals were observed for 30 min after PTZ for clonus (defined as clonic seizure of forelimbs and hind limbs during which the mouse demonstrates loss of righting). The dose of PTZ was based on estimated ED_{90} values for PTZ in these assays. The percentage of rats protected from seizure induction was assessed across doses from no effect to full protection, and the data were analyzed by Fisher's exact probability test. Comparable studies were conducted in male, TARP γ-$8^{-/-}$ and γ-$8^{+/+}$ mice[17]. Mice were treated as described for rats above except that they were given 70 mg/kg PTZ.

PTZ-induced kindled seizures and motor impairment assessments. Male CD1 mice were given PTZ (45 mg/kg, s.c.) every other day as described[30]. Mice were dosed on days 1, 3 and 5 and then divided into groups of eight or nine and tested on day 8 with either PTZ alone (45 mg/kg, s.c.), perampanel (30 mg/kg, i.p., 30 min prior) + PTZ, or LY3130481 (10 mg/kg, i.p., 30 min prior) + PTZ. Mice were then observed for 30 min for the occurrence of convulsions. Behavioral observations were conducted by a blinded but trained observer using a 3-point rating scale where 0 = no difference to vehicle side-by-side; 1 = reduced movement and/or slight gait abnormality; and/or leaning as exemplified by 100 mg/kg lamotrigine, i.p., 30 min prior; 2 = more severe aspects of rating #1 that can include falling as exemplified by 500 mg/kg valproate, i.p., 30 min prior; and 3 = marked impairment, including periodic or complete loss of righting – exemplified by 1,000 mg/kg valproate, i.p., 30 min prior. Seizure data were statistically evaluated by comparing seizure prevalence in vehicle-treated mice to drug-treated mice with Fisher's exact probability test. Behavioral data were evaluated by ANOVA with *post hoc* Dunnett's test.

Mesial temporal lobe epilepsy model. The MTLE mouse model recapitulates many of the characteristics observed in human patients with temporal lobe epilepsy (TLE). The MTLE mouse is induced by an initial neurotoxic event, a unilateral intrahippocampal injection of kainic acid (KA) into the dorsal hippocampus, which induces nonconvulsive s.e.m. lasting several hours. This initial event is followed by a latent phase. 2 to 3 weeks after KA injection, spontaneous recurrent hippocampal paroxysmal discharges (HPD) are recorded in the epileptic hippocampus and remain stable and stereotyped for the whole life of the animal[18,31]. These HPDs occur spontaneously about 30–60 times per hour when the animals are in a state of quiet wakefulness, generally last 15–20 s and are associated with behavioral arrest and/or mild motor automatisms. Adult male C57BL/6 mice were stereotaxically injected with kainate (1 nmol in 100 nL) and implanted with one bipolar electrode into the dorsal hippocampus, and then allowed to recover for 4 weeks. A dose effective against 6-Hz-induced seizures of LY3130481 was then evaluated in four MTLE mice. Each mouse was used as their own control (vehicle). Digital EEG recordings were performed on freely moving animals for a 20-min pre-injection reference period and 90-min post-dosing. Data were analyzed for the period of 10 min before and 10 min after peak time of effect of LY3130481 as observed in the 6-Hz model (15 min). Any accompanying effect on animal behavior was recorded. Data are presented as the raw number of HPDs during the analyzed 20-min period (10 min before and 10 min after) and expressed as mean ± s.e.m. and were statistically evaluated by Student's *t* test.

Inverted screen test. Sedative and ataxic effects were evaluated as described. Briefly, 30 min after LY3130481 application, but before dosing the animals with PTZ, an inverted screen test was carried out as described[4]. The apparatus is made of six 11-cm × 14-cm (mouse) or four 13-cm × 16-cm squares (rat) of round hole, perforated, stainless steel mesh (18 holes/square inch, 3/16-inch diameter, 1/4-inch staggered centers, 50% open area) that are mounted 15 cm apart on a metal rod, 35 cm above the tabletop. On the day before the test, mice were placed on the screen, and the rod was rotated 180° for 2 to 3 s. The amount of time it took for the test animal to climb to the top of the screen was recorded. For the test animals that hung on the bottom for the maximum of 60 s, a 60-s score was recorded. A test with compound on board was studied the next day in the same manner. Animals were dosed orally with the LY3130481

or intraperitoneally with GYKI52466 or perampanel and returned to their home cage. 25 min after pretreatment, the animals were tested on the inverted screen and were scored after 60 s as follows: 0 = climbed over, 50 = hanging on to screen and 100 = fell off. After the inverted screen test, animals were dosed with PTZ in a volume of 1 ml/kg and placed in an observation cage (40.6 × 20.3 × 15.2 cm) with a floor containing 0.25 inches of wood-chip bedding material. Mean ± s.e.m. data were analyzed by ANOVA and individual contrasts were evaluated by *post hoc* Dunnett's test.

Locomotor-activity assessments. Male CD1 mice were injected (i.p.) with vehicle, LY3130481 or perampanel and then evaluated for locomotor-activity changes for 45 min post-dosing. Activity was accessed in a translucent polypropylene (40.6 × 20.3 × 15.2 cm, no bedding) cage. Distance traveled and vertically directed behaviors were measured by the breaking of photo-beams (San Diego Instruments). Data were analyzed by ANOVA followed by *post hoc* Dunnett's tests. Adult, male Wistar rats (4–8 month old) were anesthetized and surgically prepared with an abdominally implanted miniature transmitter (PDT4000 Starr Life Sciences) that permitted chronic recording of body motion[32,33]. Locomotor activity of the rat in its individual home cage was monitored by telemetry signals detected using a radio-telemetry receiver located beneath the cage (ER-4000, Minimitter), and activity of the animal was tracked for 19 h. The accumulated counts were collected using SCORE-2004 software and compared to vehicle controls. Statistical significance was calculated by analysis of covariance (ANOVA) using the corresponding pre-dose baseline period as the covariate. Drug-mediated effects were measured after oral administration of LY3130418 or perampanel.

Amygdala kindling. Male Wistar rats were prepared with bipolar electrodes aimed at one hemisphere of the basolateral amygdala (AP −2.2, ML −4.8, DV −8.5 mm, relative to bregma) for electrical stimulation and EEG recording. After postoperative recovery, electrical kindling began, where a subthreshold constant current (400 μA, 1 ms, monophasic square-wave pulses, 60 Hz for 1 s) was given once a day, Monday to Friday, for 4–6 weeks until a rat was fully kindled. These rats began kindling at ~9 weeks of age at ~300 g. At the time of testing with LY3130481, the animals were ~26 weeks old and 450–500 g. A fully kindled rat has experienced ten consecutive stage 5 seizures or 10 of its last 12 were stage 5, according to the Racine scale[34]. Of the 12 fully kindled rats so developed, eight rats were selected and randomized to initial compound treatment groups. On test day, rats were dosed LY3130481 (i.p.) 30 min before stimulation with 400-μA current. The percentage of the eight rats not exhibiting seizures was assessed post stimulation. Valproic acid (300 mg/kg, i.p.) was used as a positive control. These quantal data were analyzed with Fisher's exact probability test for significance at $P < 0.05$.

Immunoprecipitation. Twenty micrograms of GluA2 antibody (NeuroMab, clone L21/32) was covalently conjugated onto the magnetic beads with Protein A and Protein G as follows. Equal volume (80 μl each) of Dynabeads Protein A and Protein G (Life Technologies) were washed with PBS and then incubated with 20 μg of the GluA2 antibody for >8 h with gentle mixing at 22 °C. The beads were washed with citrate-phosphate buffer at pH 5.0, and then with 0.2 M triethanolamine pH 8.2. The antibodies on Protein A/G were cross-linked with 20 mM DMP (dimethyl pimelimidate × 2 HCl) in 0.2 M triethanlamine, pH 8.2 for 30 min at 22 °C. The reaction was chased by the incubation with 50 mM Tris pH 7.5 for >15 min. The beads were washed by PBS containing 0.01% Tween-20. Post-nuclear P2 pellet from 1 g of rat hippocampi was prepared as described[24]. The P2 pellet was resuspended in 20× original tissue volume of PBS, and aliquoted (2 ml). AMPA-receptor antagonists were added (LY3130481: 10 μM, GYKI: 40 μM, or NBQX: 20 μM), membranes were solubilized (1% CHAPS at 4 °C for 1 h), and unsolubilized materials were removed by centrifugation (100,000*g* at 4 °C for 1 h). The resultant supernatant was incubated with magnetic beads with the anti-GluA2 (1 μg antibody) for 2–3 h. The beads were washed three times with PBS + 1% CHAPS containing the corresponding AMPA receptor antagonist. The immunoprecipitated proteins were eluted with 20 μl of Laemmli buffer without reducing reagent at 55 °C for 30 min to minimize antibody contamination. The eluted samples were reduced with DTT and then subjected to immunoblotting with anti-GluA1 (Millipore, AB1504), anti-γ-8 (Frontier Institute, TARP-g8 Rb Af1000), or anti-TARP (Upstate, 07-577) antibodies.

Data availability. All data supporting this study are provided in full in the main text of this paper and accompanying supplementary information.

22. Sommer, B. *et al.* Flip and flop: a cell-specific functional switch in glutamate-operated channels of the CNS. *Science* **249**, 1580–1585 (1990).
23. Burgess, D.L., Gefrides, L.A., Foreman, P.J. & Noebels, J.L. A cluster of three novel Ca^{2+} channel gamma subunit genes on chromosome 19q13.4: evolution and expression profile of the gamma subunit gene family. *Genomics* **71**, 339–350 (2001).
24. Kato, A.S., Siuda, E.R., Nisenbaum, E.S. & Bredt, D.S. AMPA receptor subunit-specific regulation by a distinct family of type II TARPs. *Neuron* **59**, 986–996 (2008).
25. Rouach, N. *et al.* TARP gamma-8 controls hippocampal AMPA receptor number, distribution and synaptic plasticity. *Nat. Neurosci.* **8**, 1525–1533 (2005).
26. Miledi, R., Eusebi, F., Martínez-Torres, A., Palma, E. & Trettel, F. Expression of functional neurotransmitter receptors in *Xenopus* oocytes after injection of human brain membranes. *Proc. Natl. Acad. Sci. USA* **99**, 13238–13242 (2002).
27. Miledi, R., Palma, E. & Eusebi, F. Microtransplantation of neurotransmitter receptors from cells to *Xenopus* oocyte membranes: new procedure for ion channel studies. *Methods Mol. Biol.* **322**, 347–355 (2006).
28. Eusebi, F., Palma, E., Amici, M. & Miledi, R. Microtransplantation of ligand-gated receptor-channels from fresh or frozen nervous tissue into *Xenopus* oocytes: a potent tool for expanding functional information. *Prog. Neurobiol.* **88**, 32–40 (2009).
29. Kato, A.S. *et al.* New transmembrane AMPA receptor regulatory protein isoform, gamma-7, differentially regulates AMPA receptors. *J. Neurosci.* **27**, 4969–4977 (2007).
30. Kaminski, R.M., Witkin, J.M. & Shippenberg, T.S. Pharmacological and genetic manipulation of kappa opioid receptors: effects on cocaine- and pentylenetetrazol-induced convulsions and seizure kindling. *Neuropharmacology* **52**, 895–903 (2007).
31. Suzuki, F., Junier, M.P., Guilhem, D., Sørensen, J.C. & Onteniente, B. Morphogenetic effect of kainate on adult hippocampal neurons associated with a prolonged expression of brain-derived neurotrophic factor. *Neuroscience* **64**, 665–674 (1995).
32. Harkin, A., O'Donnell, J.M. & Kelly, J.P. A study of VitalView for behavioural and physiological monitoring in laboratory rats. *Physiol. Behav.* **77**, 65–77 (2002).
33. Phillips, K.G. *et al.* Differential effects of NMDA antagonists on high frequency and gamma EEG oscillations in a neurodevelopmental model of schizophrenia. *Neuropharmacology* **62**, 1359–1370 (2012).
34. Racine, R.J. Modification of seizure activity by electrical stimulation. II. Motor seizure. *Electroencephalogr. Clin. Neurophysiol.* **32**, 281–294 (1972).

doi:10.1038/nm.4221